Preparation of a Microcrystalline Suspension Formulation of $Lys^{B28}Pro^{B29}$-Human Insulin with Ultralente Properties

JANE P. RICHARDS,[†,||] MARY P. STICKELMEYER,[†] BRUCE H. FRANK,[†] SUSAN PYE,[‡] MICHELLE BARBEAU,[‡] JERRY RADZIUK,[‡] G. DAVID SMITH,[§] AND MICHAEL R. DEFELIPPIS*[,†]

Contribution from *Lilly Research Laboratories, Eli Lilly and Company, Indianapolis, Indiana 46285, Diabetes and Metabolism Research Unit, Ottawa Civic Hospital, Ottawa, Ontario, Canada K1Y 4E9, Hauptman-Woodward Medical Research Institute, Inc., 73 High Street, Buffalo, New York 14203, and Roswell Park Cancer Institute, Elm and Carlton Streets, Buffalo, New York 14263.*

Received April 7, 1999. Accepted for publication June 28, 1999.

Abstract □ The monomeric analogue, $Lys^{B28}Pro^{B29}$-human insulin (LysPro), has been crystallized using similar conditions employed to prepare extended-acting insulin ultralente formulations. In the presence of zinc ions, sodium acetate and sodium chloride, but without phenolic preservative, LysPro surprisingly forms small rhombohedral crystals with similar morphology to human insulin ultralente crystals with a mean particle size of 20 ± 1 μm. X-ray powder diffraction studies on the LysPro crystals prior to dilution in ultralente vehicle ([NaCl] = 1.2 M) revealed the presence of $T_3R_3^f$ hexamers. Consistent with human insulin ultralente preparations, LysPro crystals formulated as an ultralente suspension ([NaCl] = 0.12 M) contain T_6 hexamers indicating that a conformational change occurs in the hexamer units of the crystals upon dilution of the salt concentration. The pharmacological properties of subcutaneously administered ultralente LysPro (ULP) were compared to ultralente human insulin (UHI) using a conscious dog model ($n = 5$) with glucose levels clamped at basal. There were no statistically significant differences between the kinetic and dynamic responses of ULP compared to UHI [C_{max} (ng/mL): 3.58 ± 0.76, ULP and 3.61 ± 0.66, UHI; T_{max} (min): 226 ± 30, ULP and 185 ± 42, UHI; R_{max} (mg/kg min): 11.2 ± 1.9, ULP and 13.3 ± 2.0, UHI; and T_{Rmax} (min): 336 ± 11, ULP and 285 ± 57, UHI]. Although the Pro to Lys sequence inversion destabilizes insulin self-assembly and greatly alters the time action of soluble LysPro preparations, this modification has now been found neither to prevent the formation of ultralente crystals in the absence of phenolics nor to compromise the protracted activity of the insulin analogue suspension.

Introduction

Extended-acting insulin preparations are microcrystalline suspensions that provide their protracted effect by slow dissolution of the crystals and gradual release of insulin into the blood stream. There are several approaches to formulating extended-acting insulin preparations. One example, ultralente human insulin (UHI),[1] is a zinc−insulin suspension composed predominantly of small rhombohedral crystals and characterized by an intermediate to long time−action profile. Ultralente is one of a series of insulin−zinc suspensions (lente insulins) that were developed by Hallas-Møller and colleagues who determined that the addition of zinc ions in preparations that had neutral pH and no zinc-binding ions (i.e., no phosphate or citrate) led to insulin formulations with protracted effects.[2,3] This series of zinc−insulin suspension formulations includes ultralente (crystalline insulin particles), semilente (amorphous insulin particles), and lente (a mixture of amorphous and crystalline insulin particles). A second approach to making protracted insulin preparations is to depress insulin solubility by adding basic peptides. This approach is exemplified by the product Neutral Protamine Hagedorn insulin (NPH). NPH is an intermediate-acting formulation prepared by cocrystallization of insulin with the basic peptide protamine.[4,5]

A recent study showed that the monomeric insulin analogue, $Lys^{B28}Pro^{B29}$-human insulin (LysPro), can be cocrystallized with the basic peptide protamine to form a microcrystalline suspension having a time action nearly identical to human insulin NPH.[6] The cocrystallization of LysPro with protamine requires the presence of both zinc ions and phenolic preservatives. In other work, the X-ray crystal structure of LysPro was reported.[7] The crystals were grown in the presence of both zinc ions and phenol, and LysPro was found to crystallize as $T_3R_3^f$ hexamers. The quaternary structure of LysPro was described using the T, R^f, and R nomenclature[7,8] for insulin hexamers whereby monomer subunits are named according to the conformation of the first eight amino acid residues of the B-chain. In this notation, T refers to an extended conformation, R to an α-helical conformation, and R^f to an extended conformation for the first three residues and α-helical for the remainder. These recent examples of LysPro crystal forms have demonstrated an apparent requirement for the presence of both zinc ions and phenolic preservatives to initiate crystallization, presumably due to the ability of these ligands to promote self-association. Indeed, numerous studies exploring the solution properties of LysPro have confirmed that the addition of zinc ions and phenolic preservatives overcomes the otherwise destabilizing effect on hexamer self-assembly caused by the sequence modification in the region required for dimer formation.[9−11]

The role of ligand binding and its influence on insulin self-assembly and crystallization is well-known for porcine and human insulin species.[12−16] One notable difference between these insulin species and LysPro is their ability to form discrete hexamers in the presence of zinc ions alone. For example, crystals of porcine insulin grown in the presence of zinc ions but without phenolic preservative have been shown by X-ray crystallography to be composed of T_6 hexamers.[16] Although high-resolution structural analysis of ultralente crystals has been thwarted by poor crystal diffraction characteristics and dimensions, atomic force microscopy studies confirmed the presence of insulin

* Corresponding author: Phone: 317-276-6027, fax: 317-277-0833, e-mail: defelippis_michael_r@lilly.com.
[†] Lilly Research Laboratories.
[‡] Ottawa Civic Hospital.
[§] Hauptman-Woodward Medical Research Institute and Roswell Park Cancer Institute.
[||] Current address: Baxter Hemoglobin Therapeutics, Inc., Boulder, CO 80301.

10.1021/js990107o CCC: $18.00 Published on Web 08/07/1999

hexamers in the crystal lattice.[17] Hexamers comprising ultralente crystals likely adopt T_6 or T_3R_3 conformations since these crystallizations are conducted in the presence of both zinc ions and sodium chloride, but in the absence of phenolic preservatives, as this additive will not produce the desired crystal form.[18]

The requirement for zinc ions and phenolic preservatives to induce crystal formation of LysPro offers a unique challenge to preparing an ultralente-type suspension of this analogue. Such a preparation may have a more desirable time−action profile compared to currently available extended-acting insulin suspensions, thus providing the impetus for undertaking the present study to explore the feasibility of producing ultralente LysPro (ULP). A variety of physicochemical techniques were used to characterize the solid material comprising the resulting ULP suspension to determine how the properties compare to authentic UHI. Pharmacological properties of ULP obtained using a conscious dog model are also reported.

Experimental Section

Chemicals—LysPro was manufactured by Eli Lilly and Company using recombinant DNA technology. All chemicals were pharmaceutical grade and were obtained from various suppliers. Humulin U (40 U/mL) (Eli Lilly and Company) was used as a comparator.

Preparation of Crystals and Formulation—A stock solution was prepared containing approximately 22 mg/mL LysPro. The endogenous level of zinc in the LysPro solid was supplemented by the addition of appropriate volumes of an acidic zinc oxide solution (10 mg/mL) to achieve a final zinc ion concentration of 0.24 mg/mL. The pH was lowered to 2.5−3.0 with 10% hydrochloric acid to aid dissolution of the LysPro solid. A separate buffer solution was prepared containing 21.3 mg/mL sodium acetate and 186.7 mg/mL sodium chloride. The pH of the buffer solution was adjusted empirically with 10% sodium hydroxide such that the combination of 62.5% of the LysPro solution and 37.5% of the buffer solution afforded a crystallization mixture having pH 5.5. Combination of the two solutions in the ratio indicated resulted in the immediate formation of a white, flocculent precipitate. The final crystallization mixture contained 14 mg/mL LysPro, 0.15 mg/mL zinc ions, 8.0 mg/mL sodium acetate, and 70 mg/mL sodium chloride. The glass, conical flask containing the crystallization mixture was mounted in a mixing apparatus and stirred continuously with a stainless steel paddle at 100 rpm. A small amount (<1% v/v) of human insulin seed crystals (Eli Lilly and Company) was added to the crystallization mixture shortly after combination. Small, rhombohedral crystals were visible by microscopy within 24 h. Crystallizations were allowed to proceed for 24−96 h at room temperature.

The ultralente LysPro (ULP) preparations used for animal testing were formulated to contain final concentrations of 1.4 mg/mL (40 U/mL) LysPro, 0.084 mg/mL zinc ions, 1.6 mg/mL sodium acetate, 7.0 mg/mL sodium chloride, and 1.0 mg/mL methylparaben at pH 7.3. To make the formulation, a stock diluent solution was prepared containing 1.11 mg/mL methylparaben, 0.89 mg/mL sodium acetate, and 0.077 mg/mL zinc ions. The diluent solution was mixed with the 400 U/mL ultralente LysPro concentrated suspension (ULP C/S) described above in a 9:1 ratio and adjusted to the final pH with 10% hydrochloric acid and/or 10% sodium hydroxide.

Optimization of Crystallization Conditions—The effects of four variables (zinc ion concentration, sodium acetate concentration, sodium chloride concentration, and pH) on ULP crystallization were evaluated using a full-factorial experimental design. All possible combinations of high and low values for each variable were tested, and a total of 16 trials and 4 centerpoints were performed in a randomly assigned order. The high/low concentrations for the four variables in the crystallization were 0.20 versus 0.29 mg/mL zinc ion, 4.0 versus 12.0 mg/mL sodium acetate, 40 versus 100 mg/mL sodium chloride, and pH 5.0 versus pH 6.0. Crystal morphology and time at which crystals formed were used as endpoints.

Analytical Methods—The concentration of LysPro in the solid and solution phases of the suspension was determined by HPLC. An aliquot of suspension was centrifuged and the supernatant decanted and retained for analysis. Distilled water, equal to the original volume of the suspension, was added to wash the pellet. The pellet was suspended and centrifuged, and the supernatant from the wash was discarded. This water wash procedure was repeated three times. After the final wash, the pellet was dissolved in a volume of 0.01 N hydrochloric acid equal to the volume of the original sample and 3 μL of 9.6 N hydrochloric acid per milliliter of solution. The dissolved pellet and supernatant fraction were analyzed with a reversed phase gradient method using a mobile phase of sulfate buffer and acetonitrile (pH 2.3), a C18 column (Spherisorb ODSII, 10 cm × 4.6 mm) temperature controlled at 40 °C and UV detection at 214 nm.

Microscopy and Particle Size Determinations—Crystal morphology was evaluated using a Zeiss Axioskop microscope equipped with a differential phase-contrast accessory. Approximately 5 μL of a resuspended sample was placed on a glass microscope slide and covered with a cover slip. Photographs were taken at 400× magnification. Edge dimensions were estimated with the aid of an ocular micrometer scale graticule subdivided into 10 μm divisions.

Particle size distributions were performed using a Coulter Multisizer and sampling stand (Miami, FL). The aperture tube orifice size was 100 μm. A 0.20 mL aliquot of resuspended sample was pipetted into 100 mL of a solution containing ISOTON II (Miami, FL). Particle size data were collected for 50 s and are reported as volume percent mean diameter ($D_{4,3}$).

Powder Diffraction—Samples were loaded into a 0.8 mm glass capillary along with mother liquor. The capillaries were then centrifuged in order to pack the microcrystals into a pellet at the bottom of the mother liquor, excess mother liquor was removed, and the capillaries were then sealed. Each capillary was placed on a Rigaku R-AXIS II-C image plate system and RU-200 rotating anode generator with graphite monochromated Cu Kα radiation (λ = 1.54178 Å) at 290 K. Following a 10- to 15-h exposure, the plot of intensity versus 2θ of the powder diffraction image was generated with the X12B software.[19] Backgrounds were subtracted from the peaks, and relative intensities were calculated for each diffraction peak. This procedure was employed for the ULP C/S prior to dilution to prepare the ULP preparation, ULP suspension (40 U/mL), and human insulin ultralente (40 U/mL).

Large, single crystals of T_6 human insulin were grown according to published procedures,[16] and a preliminary refinement of single-crystal diffraction data measured from these crystals showed the structure to be identical to that of the published structure.[16] A sample of the single crystals was ground into a fine powder in the presence of mother liquor, and the procedure described above was repeated.

As no powder diffraction data are available for the various $T_3R_3^f$ and R_6 forms of human insulin whose structures have been published,[13−15,20,21] powder patterns were simulated from the single crystal intensity data. Because of the 3-fold symmetry axis in space group *R*3, two or more general and independent reflections will make a contribution to each powder diffraction peak. Since single crystal data from protein crystals frequently have missing data, particularly at very low values of sin θ/λ, multiple sets of data for T_6 porcine[16] and human (unpublished results) insulin, $T_3R_3^f$ human insulin (chloride,[14] 4′-hydroxyacetanilide,[20] p-hydroxybenzamide[21]), and $T_3R_3^f$ LysPro[7] and a second unpublished set of data were merged using SORTAV from the DREAR suite of data reduction program package[22] to minimize missing data. Although the resulting merged data were carefully checked to ensure that there were no missing data which would alter the intensity patterns of the resulting simulated powder diffraction patterns, one strong reflection was absent from the $T_3R_3^f$ human insulin data. The merged squares of the structure factor amplitudes (F^2) were multiplied by the Lorentz and polarization factors ($Lp = (1 + \cos^2 2\theta)/(\sin^2 \theta \cos \theta)$) to give intensities corresponding to powder data. The resulting intensities were plotted as a function of 2θ after applying a broadening function to simulate the powder diffraction pattern as obtained from the R-AXIS image plate system.

$$I_{2\theta} = \sum I_{hkl} \exp - [8.66 \times (2\theta_{hkl} - 2\theta)]^2 \qquad (1)$$

Particular care must be taken in applying the correct unit cell constants in powder patterns from single-crystal intensities. Due to the relationship between the Miller indices (hkl) and the cell constants, small differences in cell constants

$$Q_{hkl} = h^2a^{*2} + k^2b^{*2} + l^2c^{*2} + 2klb^*c^*\cos\alpha^* + 2lhc^*a^*\cos\beta^* + 2hka^*b^*\cos\gamma^* \quad (2)$$

where a^*, b^*, c^*, a^*, β^*, and γ^* are the reciprocal lattice constants and

$$d = 1.0/(Q_{hkl})^{1/2} \quad (3)$$

will displace the position of the powder diffraction peak relative to nearby peaks altering the appearance of the simulated powder diffraction pattern. While single-crystal data are available for $T_3R_3^f$ LysPro human insulin,[7] no data are available for the T_6 form. As a result of the T → R conformational transition in human insulin, the a-dimension in the unit cell decreases from 81.91 to 80.83 Å while the c-dimension increases from 34.13 to 37.76 Å. It should also be noted that due to the sequence inversion in LysPro, the a-dimension in the $T_3R_3^f$ form decreases by 2.29 Å relative to that of human insulin. To a first approximation, it is possible to calculate the expected cell dimensions for T_6 LysPro based upon the observed changes in cell dimensions of human insulin.

$$a(T_6\ \text{LysPro}) = a(T_3R_3^{\,f}\ \text{LysPro}) \times [a(T_6\ \text{human})/a(T_3R_3^{\,f}\ \text{human})] \quad (4)$$

$$c(T_6\ \text{LysPro}) = c(T_3R_3^{\,f}\ \text{LysPro}) \times [c(T_6\ \text{human})/c(T_3R_3^{\,f}\ \text{human})] \quad (5)$$

In this way, a simulated powder pattern can be calculated for T_6 LysPro using expected T_6 cell constants for LysPro and intensities from human insulin.

Pharmacology—The pharmacokinetic and pharmacodynamic properties of UHI and ULP were assessed following previously described procedures.[6] Briefly, five normal conditioned mongrel dogs weighing 15−25 kg each underwent one study with ULP and one with UHI. For each animal, an 18 h fast was followed by three basal samples, a somatostatin infusion (0.3 μg/kg min), and, after a 10 min interval, a 0.5 IU/kg subcutaneous dose of either ULP or UHI. Plasma glucose was monitored at approximately 5 min intervals, and 20% glucose was infused continuously and at a variable rate to maintain near basal fasting glycemia. Additional samples were collected approximately every 5 min for 45 min, every 10 min for 40 min, every 15 min for 30 min, every 20 min for 40 min, every 25 min for 150 min, and then every 30 min until 840 min. Plasma insulin was determined by radioimmunoassay and glucose using the glucose oxidase method.

Interpolated plasma insulin and glucose profiles were compared using analysis of variance with time as a repeated measure. An overall comparison was made between the two groups (ULP and UHI), as well as of the interaction between group and time. Kinetic and pharmacodynamic parameters were compared using paired t-tests. The following parameters were evaluated for the interpolated insulin curves: C_{max}, the maximal insulin or LysPro concentration reached following its subcutaneous injection during the clamp study; T_{max}, the time at which C_{max} was attained; insulin area, the area under the insulin or LysPro curve, deemed to be representative of the total amount of exogenous insulin or LysPro which is absorbed during the course of the study; R_{max}, the maximal rate of glucose infusion which was achieved during the course of the clamp and T_{Rmax}, the time at which R_{max} was achieved. The cumulative rate of glucose infusion was also calculated. All data are reported as means ± SEM.

Results

Preparation and Characterization of ULP—The ULP preparation was prepared following a similar method used to produce ultralente (bovine, human, or porcine) insulin suspensions.[18] The procedure essentially involves preparing two solutions: an acidic protein solution containing excess zinc, and a separate precipitation solution containing sodium acetate and sodium chloride. The precipitation solution pH was appropriately adjusted to achieve crystallization conditions around the isoelectric point of LysPro (pI = 5.5). Upon combination of the protein and precipitation solutions, a flocculated, white precipitate immediately formed. Evaluation of the crystallization mixture by microscopy indicated that small rhombohedral crystals formed within 24 h; however, crystal growth was allowed to continue for up to 96 h to completely transform any remaining amorphous material. Although ULP crystals were observed to form in the absence of seed crystals (data not shown), a small amount of human insulin seed crystals (<1% v/v) were added to the crystallization reaction to improve the uniformity of the crystallization.[23] The addition of seed crystals was also noted to decrease the time required for complete crystallization.

Crystallization was routinely halted after 96 h by diluting the crystallization mixture into a diluent solution containing methylparaben. A dilution to 40 U/mL was prepared to match the concentration of the comparator UHI sample. The size and morphology of the ULP crystals comprising the suspension were evaluated by microscopy and found to be very similar to those contained in the UHI sample (data not shown). The ULP crystals were estimated to have edge lengths of approximately 5−15 μm. Mean particle size for the crystals was determined to be 20 ± 1 μm as measured by the Coulter particle size technique (data not shown). This result is in good agreement with the mean particle size of the commercial UHI sample. The completeness of crystallization in the final formulated preparation was assessed by comparing the amounts of LysPro in the solid and solution phases. Reversed-phase HPLC analysis revealed that the solid phase contained approximately 40 U/mL of LysPro whereas less than 0.05 U/mL of LysPro was found in the soluble fraction.

The conditions for preparing ULP crystals were further evaluated using a standard four-variable, full-factorial experimental design. The effects of zinc concentration, sodium acetate concentration, sodium chloride concentration, and pH were studied, and the results are summarized as follows: (i) pH had a very pronounced effect on ULP crystallization with pH 5.5 being optimal; (ii) no crystals formed at pH 5.0, regardless of the other conditions, and although some crystallization occurred at pH 6.0, these crystals were typically small, slow-growing and of poor quality compared to the crystals grown at pH 5.5; (iii) sodium acetate concentrations had little effect on crystallization within the parameters of the current experiments; (iv) an interaction between zinc and sodium chloride concentration was observed; that is, the effect of zinc concentration on crystallization depends on the sodium chloride concentration; (v) the centerpoint conditions (i.e., those closely matching the procedure for preparing UHI) reproducibly formed the highest quality crystals characterized by rhombohedral morphology with uniform size and well-defined edges forming within 24−48 h.

To characterize further the ULP suspension and possibly identify the nature of the LysPro hexamers comprising the crystals, powder diffraction studies were performed. X-ray powder diffraction has been used for many years as a means of identifying organic and inorganic microcrystalline samples. The d-spacing and intensity can be calculated for each diffraction line, and the resulting information provides an accurate and reproducible fingerprint of the material in question. This method can also be used to distinguish between different crystalline polymorphs of the same compound. While powder diffraction has rarely been applied to proteins due to lack of sufficient microcrystalline material and the requirement that the protein remain

Table 1—2θ and Relative Intensity Data Derived from Powder Diffraction Patterns[a]

ULP	UHI	T_6KP	T_6	T_6HI	$T_3R_3^f$KP	$T_3R_3^f$HI	ULP C/S	R_6R	R_6M
								b	2.10(19)
2.25(100)	2.24(81)	2.18(81)	2.17(67)	2.16(86)	2.22(100)	2.18(3)	2.25(63)		
									2.48(28)
					2.66(18)	2.66(15)	2.71(27)		
c	2.92(3)b	2.88(3)	2.88(3)b	2.88(3)					
									3.24(69)s
					3.46(50)	3.44(60)	3.50(48)		3.46(97)
3.63(13)	3.67(58)	3.78(36)a	3.68(36)	3.70(43)	3.84(5)	3.78(22)	3.85(8)		
					4.12(11)	4.08(22)	4.12(12)	4.02(11)	
4.28(17)s	4.32(52)	4.24(12)	4.19(13)	4.22(14)					4.20(46)
4.44(23)					4.44(4)	4.38(8)	4.40(4)	4.43(19)	
					4.87(3)s				4.88(46)
5.29(76)	5.22(100)	5.24(73)	5.15(82)	5.18(77)	5.18(60)	5.12(73)	5.18(62)	5.10(100)	5.14(64)
								5.54(51)	
5.77(32)	5.71(86)	5.78(60)	5.65(58)	5.70(66)	5.82(42)	5.76(90)a	5.80(87)		5.70(99)
6.12(47)	6.10(66)	6.13(41)	5.98(30)a	6.08(36)				5.94(63)	
								6.36(82)	6.26(87)a
					6.58(66)	*d*	6.60(100)	6.61(30)s	
6.88(44)	6.88(77)	6.90(100)	6.82(100)a	6.86(100)a		6.76(13)s			6.74(27)
7.26(11)		7.18(28)s			7.22(24)	7.10(38)	7.16(35)	7.08(27)	
7.60(13)	7.48(19)	7.56(15)	7.44(13)	7.48(16)		7.58(46)	7.66(40)	7.64(50)	7.46(100)a
	7.81(49)		7.71(27)	7.78(30)	7.70(24)				
8.02(20)	8.05(16)s	7.90(27)	8.02(13)	8.06(19)	8.00(44)	7.92(80)	8.01(85)a	7.98(78)	
		8.14(18)s			8.28(21)s	8.31(38)		8.36(32)	8.20(96)
8.53(3)s	8.67(32)		8.58(32)	8.64(37)	8.54(14)				
8.80(18)		8.74(34)						8.88(65)	8.74(61)
			9.09(23)	9.16(30)	9.14(35)	9.06(70)	9.14(54)		9.08(71)
9.33(24)	9.23(47)	9.26(30)	9.30(30)	9.40(31)				9.46(62)a	9.36(56)
	9.40(45)								
9.66(29)	9.71(27)	9.56(31)a	9.61(27)	9.66(27)	9.66(47)	9.54(100)	9.62(81)		
			9.80(22)s	9.90(23)					9.72(75)a
10.21(6)	10.14(19)	10.07(24)a	10.07(15)	10.12(20)	10.17(11)	10.02(26)	10.18(17)s	10.15(64)	10.22(75)a
			10.39(5)	10.44(8)b	10.40(12)	10.34(23)s	10.45(25)s		
	10.50(9)	10.66(9)	10.71(8)		10.73(13)	10.58(37)	10.66(29)	10.68(14)	
10.81(4)				10.80(9)					
						10.97(13)s			
			11.14(8)	11.24(12)s	11.29(8)a	11.07(13)s		11.06(9)	11.25(27)
				11.45(16)			11.44(19)	11.34(12)	
	11.34(12)b	11.39(12)	11.36(2)			11.33(24)			
11.68(4)		11.58(16)						11.72(16)	11.66(22)
					11.95(11)	11.82(20)	11.92(13)		
12.33(5)	12.17(23)	12.33(19)	12.04(13)	12.15(20)		12.24(25)	12.33(19)	12.08(17)	12.20(22)

[a] 2θ (degrees) and relative intensities (in parentheses) for the four measured powder diffraction patterns and the six simulated powder diffraction patterns. Codes are as follows: **ULP**, observed powder pattern for LysPro Ultralente in the presence of 7 mg/mL NaCl; **UHI**, observed powder pattern for human insulin Ultralente in the presence of 7 mg/mL NaCl; **T_6KP**, simulated powder pattern for T_6 LysPro; **T_6**, observed powder pattern for T_6 human insulin; **T_6HI**, simulated powder pattern for T_6 human insulin; **$T_3R_3^f$KP,** simulated powder pattern for $T_3R_3^f$ LysPro; **$T_3R_3^f$HI**, simulated powder pattern for $T_3R_3^f$ human insulin; **ULP C/S**, observed powder pattern for LysPro Ultralente in the presence of 70 mg/mL NaCl; **R_6R**, simulated powder pattern for the rhombohedral R_6 human insulin; and **R_6M**, simulated powder pattern for the monoclinic R_6 human insulin. A broad peak is designated by the letter b following the intensity; a shoulder on a larger peak by s; and an asymmetric peak by a. [b] Low angle data were not measured for the rhombohedral R_6 human insulin structure. [c] There is a very small broad peak at this value of 2θ, but its intensity is too small to estimate. [d] The (–3,4,2) reflection which comprises 99% of the intensity of this peak was not measured in the human insulin data.

immersed in its mother liquor, it is certainly capable of identifying various polymorphs by changes in *d*-spacings and intensities of the resulting powder pattern. In the case of crystals of hexameric insulin, the low resolution powder lines ($0° < 2\theta < 12°$) provide a definitive way in which to identify the hexamer type within a crystal due to significant differences in the unit cell constants of the three different hexamer types, T_6, $T_3R_3^f$, and R_6.

The powder diffraction results are summarized in Table 1 where the 2θ values and relative intensities are listed for the measured and simulated powder patterns obtained for the various insulin forms. An examination of the simulated powder patterns for the rhombohedral or monoclinic R_6 forms shows no similarity to that of the observed powder patterns for UHI, either of the ULP samples (concentrated or diluted) or T_6 human insulin. Neither is there any similarity of the R_6 forms to the simulated powder patterns for T_6 or $T_3R_3^f$ LysPro or human insulin. Therefore, it is clear that neither of the ultralente forms possess R_6 hexamers in either rhombohedral or monoclinic unit cells.

A comparison of the simulated and observed powder patterns for T_6 human insulin showed that they are in quite good agreement in both 2θ and intensities for each peak, suggesting that preferred orientation is not a serious problem. As noted earlier, some care must be taken in comparing the powder patterns from human insulin to that of LysPro, since the small changes in unit cell constants are sufficient to alter the 2θ values of certain diffraction peaks.

With one exception, a very strong diffraction peak is observed at a 2θ value of approximately 2.20° for all T_6 or $T_3R_3^f$ samples. This strong peak has Miller indices of (−2,1,0) and is a consequence of rows of insulin hexamers spaced 40.2 Å apart and perpendicular to the *a*- and *b*-axes. The presence of this strong peak in the unknown ultralente diffraction patterns is indicative of the presence of hexam-

ers in the crystals. The one exception is that of $T_3R_3^f$ human insulin, but in this case, due to the very low value of θ, a portion of the peak was obscured by the beam stop during the measurement of the data.

While there are similarities in the 2θ values for the crystals containing either T_6 or $T_3R_3^f$ hexamers, there are several peaks which are quite characteristic of one or the other forms. For example, peaks at average 2θ values of 2.66, 3.45, 4.10, and 6.58° are only observed in the simulated powder patterns for $T_3R_3^f$ human insulin or $T_3R_3^f$ LysPro. Likewise, peaks at 2.88, 4.22, 6.06, and 9.32° are only observed in the simulated powder patterns for T_6 human insulin. Therefore, these peaks can be used as a very sensitive indicator of the conformation of the hexamer present in the unknown ultralente samples.

An examination of the observed powder pattern for ULP C/S grown in the presence of 70 mg/mL sodium chloride shows that it contains peaks at 2.71, 3.50, 4.12, and 6.60°, but none at 2.88, 4.22, 6.06, and 9.32° 2θ. Thus, the powder diffraction pattern clearly identifies this sample to be made up of $T_3R_3^f$ hexamers. In contrast, the observed powder patterns for ULP and UHI having sodium chloride concentrations of 7 mg/mL contain peaks at 2.92, 4.30, 6.11, and 9.28°, but none at 2.66, 3.45 or 4.10, or 6.58° 2θ, which is completely consistent with the presence of a T_6 hexamer in the crystal structure.

Pharmacological Characterization—ULP was compared to UHI with respect to both its plasma concentration and glucose requirements following subcutaneous injection. During the study, glucose concentrations were monitored, and its intravenous infusion was adjusted to maintain near-basal concentrations (a clamp procedure). The rate of glucose infusion, in turn, defines the action of insulin administered. For UHI, the basal (fasting, preexperimental) glucose concentration was 109 ± 3 mg/dL. Hourly glucose concentrations thereafter were 116 ± 5, 118 ± 8, 120 ± 7, 117 ± 2, 110 ± 2, 117 ± 4, 112 ± 3, 112 ± 2, 117 ± 3, 115 ± 4, 111 ± 1, 118 ± 3, and 111 ± 5 mg/dL. For ULP, the basal glucose concentration was 105 ± 2 mg/dL with hourly concentrations of 113 ± 6, 110 ± 5, 110 ± 6, 111 ± 5, 105 ± 6, 116 ± 6, 113 ± 6, 113 ± 4, 111 ± 6, 114 ± 5, 114 ± 5, 113 ± 6, and 111 ± 3 mg/dL. There was no difference between the two groups ($F = 0.47$ and $p = 0.51$) or any divergence between them in time ($F = 0.80$ and $p = 0.55$). The stability of the clamp procedure was indicated by the absence of change in the glucose level over time ($F = 1.78$ and $p = 0.15$).

Figure 1 shows the insulin and LysPro concentrations following the subcutaneous injection of the UHI and ULP preparations. The profile of the two curves is similar, and the LysPro concentrations appear to be slightly higher. Analysis of variance, however, indicates that the two curves are not distinguishable ($F = 0.94$ and $p = 0.36$), nor do they diverge in time ($F = 0.31$ and $p = 0.77$). Within the limits of the current study, there are no discernible differences between the responses of the two preparations. The concentration profiles were found to decrease to between 20 and 40% of peak values by the end of the study (14 h after injection). As shown in Table 2, the average maximal concentration (C_{max}) of human or LysPro achieved in these studies is similar (approximately 3.6 ng/mL). The time at which these peaks occur is also not different (approximately 200 min), and the area under the curves remains analogous at ~1500 ng-min/mL. Within the bounds of this comparison, there are no differences in the kinetic parameters examined.

The rate of glucose infusion necessary to maintain fasting glycemia is shown in Figure 2. Inspection of the data reveals an almost identical pattern of glucose infusion over the course of the study. On the basis of statistical

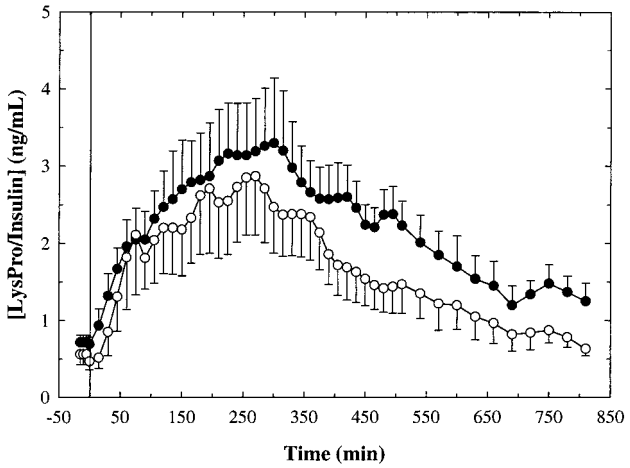

Figure 1—Plasma human insulin or LysPro concentrations following administration of subcutaneous injections of either commercial UHI (○) or ULP suspension (●) at time zero. The dose used was 0.5 U/kg. Concentrations were measured using radioimmunoassays. Error bars represent the average of five test animals.

Table 2—Pharmacokinetic and Pharmacodynamic Parameters Following Subcutaneous Administration of UHI and ULP (means ± SEM)

parameter	UHI	ULP	*T*	*p*
C_{max} (ng/mL)	3.61 ± 0.66	3.58 ± 0.76	0.074	0.94
T_{max} (min)	185 ± 42	226 ± 30	–0.97	0.39
insulin area (ng-min/mL)	1340 ± 257	1760 ± 305	–1.38	0.24
R_{max} (mg/kg-min)	13.3 ± 2.0	11.2 ± 1.9	1.06	0.35
T_{Rmax} (min)	285 ± 57	336 ± 11	–0.94	0.40
total glucose infused[a] (g/kg)	4.95 ± 0.70	4.20 ± 0.70	1.086	0.34

[a] Total glucose infused until $t = 840$ min.

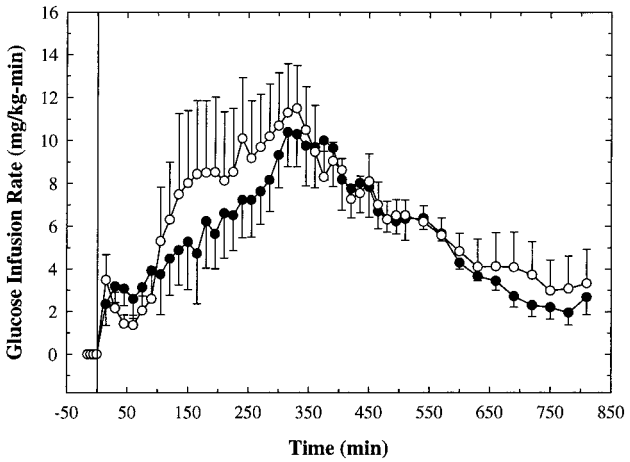

Figure 2—Rates of glucose infusion necessary to maintain fasting glycemia during the glucose clamp imposed following subcutaneous injection of either commercial UHI (○) or ULP suspension (●). The dose used was 0.5 U/kg. Plasma glucose concentrations were measured using a glucose oxidase method. Error bars represent the average of five test animals.

analysis, there is no indication of either an overall group difference or any divergence of the behavior of the groups in time (analysis of variance results: group, $F = 1.77$ and $p = 0.24$; time, $F = 3.81$ and $p = 0.06$; group *x* time, $F = 0.94$ and $p = 0.42$). Both preparations yield very similar peaks approximately 5 h after injection and decrease thereafter until 14 h. The profiles are therefore essentially identical. A plot of the cumulative amount of glucose infused following subcutaneous administration is shown in Figure 3. This cumulative amount is obtained by integrating the glucose infusion curves. Inspection of these data

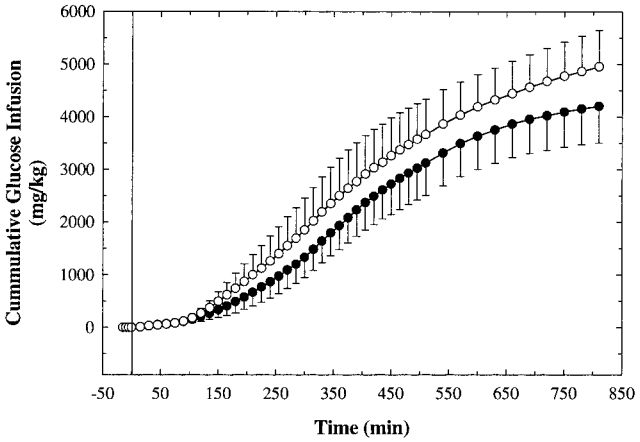

Figure 3—Cumulative glucose infusion following subcutaneous injection of either commercial UHI (○) or ULP suspension (●). Results are based on the integration of the curves shown in Figure 2. Error bars represent the average of five test animals.

show the consistent result that the ultralente preparations of human insulin and LysPro require very similar amounts of glucose to cover their subcutaneous injections. The pharmacodynamic parameters calculated were the maximum rate of glucose infusion (R_{max}), the time at which this was achieved (T_{Rmax}), and the total amount of glucose infused over 14 h and are shown in Table 2. Corroborating the comparison of the curves of glucose infusion, these parameters are all statistically equivalent. Maximal glucose infusion rates are ~12 mg/kg-min and are reached at approximately 5 h after injection of either preparation. A total of about 4.5 g/kg of glucose is infused in each case.

Discussion

LysPro Crystallizes in the Absence of Phenolic Preservatives—On the basis of the wealth of X-ray crystallographic data on wild-type insulins (bovine, human, and porcine), it is clear that the crystals are composed of precisely oriented hexamer units. Studies on the precrystallization stage of 2Zn-porcine insulin further demonstrated that crystal growth proceeds by the addition of hexamers, indicating the importance of solution state self-association to crystallization.[24] Because the wild-type insulin species are known to self-associate into well-defined hexamers in the presence of zinc ions alone, the preparation of ultralente suspensions is straightforward. In contrast, LysPro aggregates nonspecifically in the presence of zinc ions, producing high molecular weight species[11] suggesting that crystallization is unlikely to proceed without modification to the ultralente procedure. We hypothesized that the inclusion of a phenolic preservative in the crystallization media might be necessary, as it is known that LysPro will form well-defined hexamers in the presence of both this ligand and zinc ions.[9,11] Indeed, previous studies describing the preparation of NPH crystals of LysPro demonstrated the necessary requirement of producing LysPro hexamers by the addition of both zinc ions and phenol prior to initiating crystallization.[6]

Contrary to the expected outcome, ultralente crystals of LysPro did form in the absence of phenolic preservative with a procedure similar to that used for wild-type insulins. The fact that LysPro forms crystals with morphology and dimensions indistinguishable from human insulin ultralente crystals suggests that the concentrations of zinc and halide ions override the destabilizing effects of the Pro,Lys amino acid inversion driving the formation of LysPro hexamers. The high sodium chloride concentration (1.2 M) used in the crystallization media may also serve to inhibit nonspecific high-order aggregation by an electrostatic effect.

Evidence for a $T_3R_3^f \rightarrow T_6$ Structural Transformation—Powder diffraction studies revealed that both the ULP and UHI formulations are composed of crystals containing T_6 hexamers. While $T_3R_3^f$ crystals of LysPro have been previously prepared, this is the first report demonstrating the crystallization of LysPro as T_6 hexamers. Furthermore, our studies provide definitive data on the nature of the crystals comprising UHI suspensions. Such information has heretofore been inaccessible due to the poor diffraction quality of the crystals. We also note that the presence of methylparaben in either the ULP or UHI formulations does not affect hexamer conformation (i.e., inducing the T → R transition). In contrast to the T_6 hexamer conformation identified in the ultralente formulations, the ULP C/S sample was found to contain $T_3R_3^f$ hexamers.

While it may appear that the differences between the two LysPro ultralente samples present an anomaly, since one is T_6 and the other $T_3R_3^f$, there is a simple explanation for this behavior. Diffraction quality single crystals of insulin have been transformed from T_6 to $T_3R_3^f$ by reducing the sodium chloride content to less than 0.3 M,[25,26] and a similar transformation can be effected from R_6 to $T_3R_3^f$ by reducing the phenol concentration (unpublished results). Single crystals treated in such a fashion still retain their diffraction properties despite the occurrence of the R → T transition in the crystal structure. In this study, the dilution of the sodium chloride concentration from 1.2 to 0.12 M as formulated for animal testing is sufficient to induce the R → T transition, resulting in a crystalline powder sample made up of T_6 hexamers. Thus, the original ULP C/S crystals grown at 1.2 M sodium chloride contain $T_3R_3^f$ hexamers, and the dilution to 0.12 M sodium chloride transforms these crystals to T_6. These results also show that despite differences in a formulated insulin preparation as compared to the crystallizing media used to prepare diffraction quality single crystals, the formulated microcrystals possess a structure nearly identical to that obtained from single-crystal diffraction studies.

Pharmaceutical Relevance—The primary motivation for exploring the feasibility of preparing a LysPro ultralente formulation was to compare the time–action profile to that of wild-type insulin preparations. A study comparing the activity of bovine, human, and porcine ultralente showed that all preparations evaluated displayed a duration of activity in excess of 30 h.[27] However, bovine ultralente displayed a flat, essentially peakless profile although it was noted that a consistent peak was not evident due to the wide variability between subjects. The authors also concluded that any one of the ultralente formulations is suitable to provide basal insulinemia in clinical practice. Nevertheless, a peakless profile with a time–action greater than 24 h is considered highly desirable in certain diabetes treatment regimens.

Atomic force microscopy studies have provided evidence that the difference in time action between bovine ultralente compared to either human or porcine ultralente may be related to packing and orientation of insulin hexamers at the crystal–solution interface.[17] In bovine ultralente crystals, the hexamers on the predominant faces [(010) and (110)] are oriented "edge-on" to the aqueous medium, limiting solvent penetration into the crystals and consequently further retarding dissolution. Conversely, the predominant exposed crystal surface of human and porcine ultralente crystals is the (001) crystal plane. Hexamer orientation on this face allows for easier penetration of solvent through the crystal surface, contributing to more rapid dissolution. Given this diversity in ultralente crystal

morphology, it is reasonable to evaluate the pharmacological properties of insulin analogue suspensions especially in light of the inherent immunological issues associated with bovine insulin preparations.[28] The pharmacological data collected on ULP indicate that it has a time−action profile that is more consistent with human rather than bovine insulin ultralente. This result is nonetheless interesting considering the perturbed self-association properties of LysPro. Despite the "monomeric" nature of LysPro, crystallization as an ultralente form did not result in any significant decrease in duration of activity compared to UHI.

References and Notes

1. The following abbreviations are used: C_{max}, maximal insulin/LysPro concentration; LysPro, [Lys^{B28},Pro^{B29}]-human insulin analogue; NPH, Neutral Protamine Hagedorn; R_6, insulin hexamers in which the B-chain residues B1−B8 of all monomer subunits are α-helical resulting in a continuous α-helix from B1−B19; R_{max}, maximal rate of glucose infusion; T_3R_3, insulin hexamers in which three of the monomer subunits contain an extended conformation for B-chain residues B1−B8 and B9−B19 are α-helical while the other three monomers contain B-chain residues B1−B8 that are α-helical resulting in a continuous α-helix from B1−B19; $T_3R_3^f$, insulin hexamers in which three of the monomer subunits contain an extended conformation for B-chain residues B1−B8 and B9−B19 are α-helical while the other three monomers have a "frayed" α-helix in which the B-chain residues B1−B3 are extended and only B4−B19 are α-helical; T_6, insulin hexamers in which the B-chain residues B1−B8 of all monomer subunits are in an extended conformation and B9−B19 are α-helical; T_{max}, time at which C_{max} is attained; T_{Rmax}, time at which R_{max} is attained; (UHI), ultralente human insulin; ULP, ultralente LysPro; ULP C/S, ultralente LysPro concentrated suspension.
2. Hallas-Møller, K.; Petersen, K.; Schlichtkrull, J. Crystalline and Amorphous Insulin-Zinc Compounds with Prolonged Action. *Science* **1952**, *116*, 394−398.
3. Hallas-Møller, K. The Lente Insulins. *Diabetes* **1956**, *5*, 7−14.
4. Hagedorn H. C.; Jensen, B. N.; Krarup, N. B.; Wodstrup, I. Protamine Insulinate. *J. Am. Med. Assoc.* **1936**, *106*, 177−180.
5. Krayenbühl, C.; Rosenberg, T. Crystalline Protamine Insulin. *Rep. Steno Mem. Hosp. Nord. Insulinlab* **1946**, *1*, 60−73.
6. DeFelippis, M. R.; Bakaysa, D. L.; Bell, M. A.; Heady, M. A.; Li, S.; Pye, S.; Youngman, K. M.; Radziuk, J.; Frank, B. H. Preparation and Characterization of a Cocrystalline Suspension of [Lys^{B28},Pro^{B29}]-Human Insulin Analogue. *J. Pharm. Sci.* **1998**, *87*, 170−176.
7. Ciszak, E.; Beals, J. M.; Frank, B. H.; Baker, J. C.; Carter, N. D.; Smith, G. D. Role of C-terminal B-chain Residues in Insulin Assembly: The Structure of Hexameric Lys^{B28}-Pro^{B29}−Human Insulin. *Structure* **1995**, *3*, 615−622.
8. Kaarsholm, N. C., Ko, H.-C., Dunn, M. F. Comparison of Solution Structural Flexibility and Zinc Binding Domains for Insulin, Proinsulin, and Miniproinsulin. *Biochemistry* **1989**, *28*, 4427−4435.
9. Bakaysa, D. L.; Radziuk, J.; Havel, H. A.; Brader, M. L.; Li, S.; Dodd, S. W.; Beals, J. M.; Pekar, A. H.; Brems, D. N. Physicochemical Basis for the Rapid Time-action of Lys^{B28}-Pro^{B29}-Insulin: Dissociation of a Protein−Ligand Complex. *Protein Sci.* **1996**, *5*, 2521−2531.
10. Birnbaum, D. T.; Kilcomons, M. A.; DeFelippis, M. R.; Beals, J. M. Assembly and Dissociation of Human Insulin and $Lys^{B28}Pro^{B29}$-Insulin Hexamers: A Comparison Study. *Pharm. Res.* **1997**, *14*, 25−36.
11. Richards, J. P.; Stickelmeyer, M. P.; Flora, D. B.; Chance, R. E.; Frank, B. H.; DeFelippis, M. R. Self-Association Properties of Monomeric Insulin Analogues Under Formulation Conditions. *Pharm. Res.* **1998**, *15*, 1434−1441.
12. Derewenda, U.; Derewenda, Z.; Dodson, E. J.; Dodson, G. G.; Reynolds, C. D.; Smith, G. D.; Sparks, C.; Swenson, D. Phenol Stabilizes More Helix in a New Symmetrical Zinc Insulin Hexamer. *Nature* **1989**, *338*, 594−596.
13. Smith, G. D.; Dodson, G. G. Structure of a Rhombohedral R_6 Insulin/Phenol Complex. *Proteins, Struct. Funct. Genet.* **1992**, *14*, 401−408.
14. Ciszak, E.; Smith, G. D. Crystallographic Evidence for Dual Coordination around Zinc in the T_3R_3 Human Insulin Hexamer. *Biochemistry* **1994**, *33*, 1512−1517.
15. Smith, G. D.; Swenson, D. C.; Dodson, E. J.; Dodson, G. G.; Reynolds. C. D. Structural Stability in the 4-Zinc Human Insulin Hexamer. *Proc. Natl. Acad. Sci. U.S.A.* **1984**, *81*, 7093−7097.
16. Baker, E. N.; Blundell, T. L.; Cutfield, J. F.; Cutfield, S. M.; Dodson, E. J.; Dodson, G. G.; Crowfoot Hodgkin, D. M.; Hubbard, R. E.; Isaacs, N. W.; Reynolds, C. D.; Sakabe, K.; Sakabe, N.; Vijayan, N. M. The Structure of 2Zn Pig Insulin Crystals at 1.5 Å Resolution. *Philos. Trans. R. Soc. London B* **1988**, *319*, 369−456.
17. Yip, C. M.; DeFelippis, M. R.; Frank, B. H.; Brader, M. L.; Ward, M. D. Structural and Morphological Characterization of Ultralente Insulin Crystals by Atomic Force Microscopy: Evidence of Hydrophobically Driven Assembly. *Biophys. J.* **1998**, *75*, 1172−1179.
18. Brange, J.; Skelbaek-Pedersen, B.; Langkjaer, L.; Damgaard, U.; Ege, H.; Havelund, S.; Heding, L. G.; Jørgensen, K. H.; Lykkeberg, J.; Markussen, J.; Pingel, M.; Rasmussen, E. *Galenics of Insulin. The Physicochemical and Pharmaceutical Aspects of Insulin and Insulin Preparations*; Springer-Verlag: Berlin, Heidelberg, 1987.
19. Capel, M. **1998**, X12B Software, http://crim12b.nsls.bnl.gov/x12b_downloads.html.
20. Smith, G. D.; Ciszak, E. The Structure of a Complex of Hexameric Insulin and 4′-Hydroxyacetanilide. *Proc. Natl. Acad. Sci. U.S.A.* **1994**, *91*, 8851−8855.
21. Smith, G. D.; Ciszak, E.; Pangborn, W. A Novel Complex of a Phenolic Derivative with Insulin: Structural Features Related to the T → R Transition. *Protein Sci.* **1996**, *5*, 1502−1511.
22. Blessing, R. H. Data Reduction and Error Analysis for Accurate Single-Crystal Diffraction Intensities. *Crystallogr. Rev.* **1987**, *1*, 3−58.
23. Schlichtkrull, J. Insulin Crystals IV. The Preparation of Nuclei, Seeds and Monodisperse Insulin Crystal Suspensions. *Acta Chem. Scand.* **1957**, *11*, 299−302.
24. Kadima, W.; McPherson, A; Dunn M. F.; Jurnak, F. Precrystallization Aggregation of Insulin by Dynamic Light Scattering and Comparison with Canavalin. *J. Cryst. Growth* **1991**, *110*, 188−194.
25. Bentley G.; Dodson G.; Lewitova, A. Rhombohedral Insulin Crystal Transformations. *J. Mol. Biol.* **1978**, *126*, 871−875.
26. Reynolds, C. D.; Stowell, B.; Joshi, K. K.; Harding, M. M.; Maginn, S. J.; Dodson G. G. Preliminary Study of a Phase Transformation in Insulin Crystals Using Synchrotron-Radiation Laue Diffraction. *Acta Crystallogr.* **1988**, *B44*, 512−515.
27. Seigler, D. E.; Olsson, G. M.; Agramonte, R. F.; Lohman, V. L.; Ashby, M. H.; Reeves, M. L.; Skyler, J. S. Pharmacokinetics of Long-acting (Ultralente) Insulin Preparations. *Diab. Nutr. Metab.* **1991**, *4*, 267−273.
28. Schernthaner, G. Immunogenicity and Allergenic Potential of Animal and Human Insulins. *Diabetes Care* **1993**, *16*, 155−165.

Acknowledgments

We thank Maureen Bell of Eli Lilly and Company for assistance with the Coulter particle size determinations and Quovadis McKenzie (Eli Lilly and Company summer intern) for help in performing the ultralente crystallizations. Dr. Walter A. Pangborn of the Hauptman-Woodward Medical Research Institute is thanked for assistance in measuring the observed powder patterns. The authors also thank Dr. Ron Chance for critical review of the manuscript.

JS990107O